A. Alexiou
Senior Researcher
e-mail: a.alexiou@ltt.ntua.gr

A. Tsalavoutas
Senior Researcher
e-mail: ttsal@ltt.ntua.gr

Laboratory of Thermal Turbomachines,
National Technical University of Athens,
15773, Athens, Greece

B. Pons
Pre-Design Team
TURBOMECA 65411,
Bordes Cedex France
e-mail: Bernard.Pons@turbomeca.fr

N. Aretakis
Lecturer
e-mail: naret@central.ntua.gr

I. Roumeliotis[1]
Senior Researcher
e-mail: jroume@central.ntua.gr

K. Mathioudakis
Professor
e-mail: kmathiou@central.ntua.gr

Laboratory of Thermal Turbomachines,
National Technical University of Athens,
15773, Athens, Greece

Assessing Alternative Fuels for Helicopter Operation

At present, nearly 100% of aviation fuel is derived from petroleum using conventional and well known refining technology. However, the fluctuations of the fuel price and the vulnerability of crude oil sources have increased the interest of the aviation industry in alternate energy sources. The motivation of this interest is actually twofold: firstly, alternative fuels will help to stabilize price fluctuations by relieving the worldwide demand for conventional fuel. Secondly, alternative fuels could provide environmental benefits including a substantial reduction of emitted CO_2 over the fuel life cycle. Thus, the ideal alternative fuel will fulfill both requirements: relieve the demand for fuels derived from crude oil and significantly reduce CO_2 emissions. In the present paper, the effects of various alternative fuels on the operation of a medium transport/utility helicopter are investigated using performance models of the helicopter and its associated turboshaft engine. These models are developed in an object-oriented simulation environment that allows a direct mechanical connection to be established between them in order to create an integrated model. Considering the case of a typical mission for the specific helicopter/engine combination, a comparative evaluation of conventional and alternative fuels is then carried out and performance results are presented at both engine and helicopter levels. [DOI: 10.1115/1.4007169]

Introduction

Aviation currently accounts for around 2% of man-made CO_2 emissions [1]. However its contribution to total greenhouse gas emissions is higher ($\sim$3%) due to other exhaust gases and contrails emitted during flight.

Future emission levels from aviation will depend on the relative rates of growth and the scale of technological improvements. Worldwide traffic is predicted to grow at a rate of 4%-5% per year [2]. The CO_2 emissions by worldwide aviation in 2050 would be nearly six times their current level if fuel consumption grows at the same rate.

In awareness of the environmental consequences of continued CO_2 growth, IATA members have agreed in June 2009 to a set of ambitious goals:

- carbon neutral growth of aviation from 2020
- improve fuel efficiency by 1.5% the subsequent decade
- reduce CO_2 emissions by 50% by 2050 compared with 2005 levels

These targets are planned to be achieved using a four pillar strategy which includes improved technology, effective operations, efficient infrastructure, and positive economic measures [3]. Of these four pillars, technology has the best prospect for reducing aviation emissions with advances in engine configurations, aircraft/rotorcraft designs, and used materials while significant benefits will be achieved by the implementation of alternative fuels.

Sustainable biofuels can reduce aviation's net carbon contribution by almost 100% on a *full life-cycle* basis. Research is mainly focused on biofuels derived from second or new generation biomass (e.g., algae, jatropha, and camelina).

Tests [4] demonstrated that the use of biofuels as "drop-in" fuels is technically sound and does not require any major adaptation of the aircraft. To date, the aviation industry is cleared to use blends with up to 50% "synthetic" kerosene derived from coal, gas or biomass and conventional jet fuel.

In this study, the use of five alternative fuels in a medium utility helicopter is examined and compared with that of Jet-A, employing appropriate performance models of the helicopter and its turboshaft engines. Although the helicopter operations sector has currently a relatively small share of the total aviation market, its role is continuously expanding to fulfill the needs of modern society to certain modes of transport (e.g., offshore), medical assistance (air ambulances), law enforcement, search and rescue, fire-fighting, etc. Hence, its future environmental impact would be significant if measures are not taken now to reduce greenhouse gas emissions over the entire mission range.

The paper describes the approach followed to create an integrated model for helicopter mission analysis that is also capable to allow the use of different fuels. A test case is then considered for which the performance of both engine and helicopter is presented when Jet-A is the fuel used, before demonstrating the effects from using specific alternative fuels.

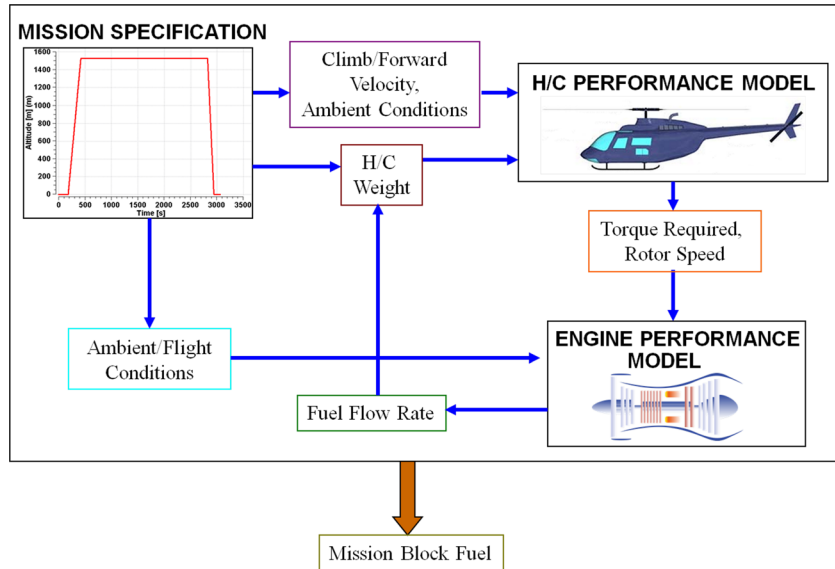[1]Also a Lecturer at the Hellenic Naval Academy, Piraeus, Greece.

Fig. 1 Module information exchange diagram

Integrated Model Description

The amount of fuel consumed by an aircraft (rotary or fixed wing) during a mission may be evaluated by coupling an engine performance model for off-design analysis with an aircraft performance model so that the following sequence of calculations can be realized:

- Define the required mission profile in terms of ambient and flight conditions.
- Determine aircraft thrust or power requirements from aircraft performance model and for the current aircraft weight and mission point.
- For a given fuel, use the engine performance model to calculate the fuel consumption corresponding to the environmental conditions and throttle setting of the current mission point.
- Update the aircraft weight and calculate the next mission point.
- Sum the fuel consumed at each point to obtain the mission block fuel burn.

This calculation sequence for a helicopter mission analysis is represented graphically in Fig. 1.

In this study, both the helicopter and engine performance models are developed in the PROOSIS v2.6.0 simulation environment [5]. This is a stand-alone, flexible and extensible object-oriented tool capable of performing steady-state and transient calculations as well as multifidelity, multidisciplinary, and distributed gas turbine engine performance simulations [6]. Different calculation types can be carried out, such as mono or multipoint design, off-design, test analysis, sensitivity, optimization, deck generation,

etc. It features an advanced graphical user interface allowing for modular model building by "dragging-and-dropping" the required component icons from one or more library palettes to a schematic window. A component icon, for example, could represent a single engine component (e.g., compressor, turbine, burner, nozzle, etc.), a subassembly, a complete engine, a control system, an aircraft model, etc. Components communicate with each other through their ports. Ports define the set of variables to be interchanged between connected components (e.g., mass flow rate, pressure, and temperature in a fluid port or rotational speed, torque and inertia in a mechanical port, etc.). The mathematical modeling of components and ports is described with a high-level object-oriented language.

For the work reported here, the TURBO library of engine components available as standard in PROOSIS is used to create the free turbine turboshaft engine model shown in Fig. 2. The library uses industry accepted performance modeling techniques and respects the international standards with regards to nomenclature, interface, and object-oriented programming. The engine model has a gas generator consisting of a twin stage centrifugal compressor (LPC and HPC) driven by a single stage axial turbine (HPT). The free power turbine (PT) is a twin axial turbine delivering shaft power through a gearbox (GBX). The model uses appropriate maps to define off-design performance for the turbomachinery components. The burner pressure losses vary with the burner inlet corrected mass flow rate while burner efficiency is a function of burner loading. Interturbine duct (DIT) and diffuser pressure losses vary with inlet swirl angle while the efficiency of the inlet depends on the inlet mass flow rate. Cooling/sealing flows for the HPT and PT components are extracted from the exit of LPC and HPC as required. Shaft and gearbox transmission losses are also
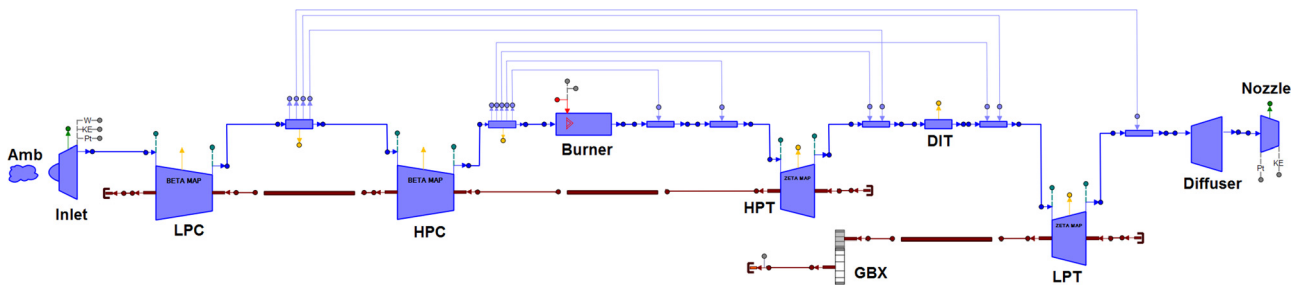

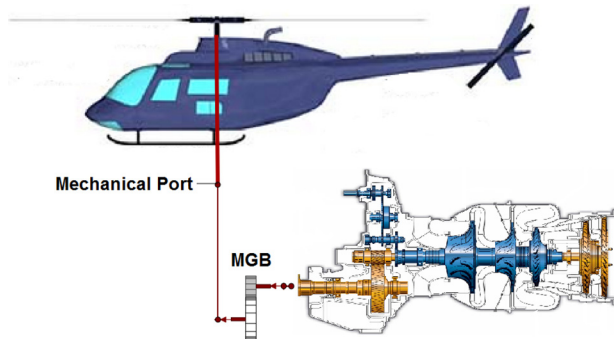**Fig. 2 Turboshaft engine PROOSIS schematic diagram**

Fig. 3 PROOSIS schematic diagram of integrated model

accounted for. Inlet and exhaust (nozzle) pressure losses, customer power, and bleed air extraction (from HPC exit) can be specified. For a given set of ambient and flight conditions, the model only needs the power required and rotational speed at the gearbox outlet shaft (assumed fixed) in order to calculate the complete cycle. The PROOSIS engine model was validated against proprietary data and tools by Turbomeca [7].

The helicopter performance model is coded as a stand-alone PROOSIS component with a mechanical port to allow it to connect with the engine performance model. The total helicopter power required is calculated according to [8] and takes into account the main rotor power, the tail rotor power, any customer power extraction needs, and the gearbox power losses. The main rotor power comprises the induced, profile, fuselage, and potential energy change power terms according to the current helicopter weight, forward and vertical velocity of the helicopter and air density at the current environmental conditions. The type of helicopter is defined through a list of attributes including the number of engines and main rotor blades, the maximum take-off weight, etc. The total power required is then divided by the number of engines to determine the torque needed by each engine for a specified rotor speed.

The integrated model is then constructed by combining in a single PROOSIS schematic diagram the engine and helicopter component icons and connecting the helicopter's outlet mechanical port to the corresponding engine's one through a component representing the helicopter main gearbox (MGB), as shown in Fig. 3. The corresponding mathematical model requires only the helicopter current weight and the forward and vertical helicopter velocities to be defined in order to solve the formulated equation system. In a mission analysis calculation, the velocities are specified (either directly or indirectly from distance traveled over a certain time) while the helicopter weight is continuously updated (starting from an initially specified value) by subtracting the weight of fuel burned during the current mission point operating conditions.

Alternative Fuel Models. It is well recognized that the implementation of alternative fuels will help to reduce the environmental impact of aviation. There are a number of different processing techniques that can be used to produce alternative fuels. At present two of them have received approval for use in aviation: the

Table 2 Engine parameters for given ratings at SL/STD

Parameter	MCP	TOP	OEI30
Power delivered (kW)	1056	1252	1437
Torque delivered (N m)	1681	1992	2287
Overall pressure ratio	11.6	12.6	13.3
Power turbine inlet temperature (K)	977	1034	1108
Inlet air mass flow rate (kg/s)	4.6	4.8	4.94
Gas generator speed (rpm)	38946	40205	41700
Specific fuel consumption (kg/kWh)	0.280	0.271	0.269

Fischer-Tropsch (FT) and the hydroprocessed esters and fatty acids (HEFA) process. The latest is also known as hydrotreated renewable jet (HRJ).

In both cases, the produced fuels have a narrower band composition, the major difference is the lack of aromatic and polyaromatic compounds. This results in a lower density as can be seen in Table 1, where some properties of the fuels considered in the present study are given. The percentage differences appearing in the brackets are relevant to Jet-A. It is observed that the densities of net synthetic jet fuels do not comply with the requirements of ASTM standard D1655 (density should be between 775 and 840 kg/m^3).

Furthermore, the industry has concerns about the low aromatics content, absence of natural anti-oxidants, low electrical conductivity, and lubrication properties of synthetic jet fuels. Issues that might arise from these abnormalities are erroneous fuel metering, accelerated wear of fuel system O-rings and seals, fuel degradation in long-term storage and high pressure fuel pump wear, as well as increased fire hazard.

Currently the production and implementation of alternative fuels is covered by the ASTM standard D7566 which states that synthetic blending components are not satisfactory for aviation engines unless blended with conventional fuel. Namely, blends with up to 50% FT-SPK or 50% HRJ-SPK can be used.

The TURBO library in PROOSIS uses three-dimensional linearly interpolated tables for calculating the caloric properties of the working fluid in the engine model. These are generated with the NASA CEA software [12] for each of the fuels considered. Dissociation of combustion products is not taken into account (maximum cycle temperature is below 1500 K). It is noted that even though biodiesels are not approved for aviation use, they are included in the present study for comparative purposes.

Case Study. Using the integrated model described in the previous section the case of a medium transport/utility helicopter is considered for studying the effects of using the alternative fuels presented in Table 1. The analysis starts by presenting the engine and helicopter performance when Jet-A is used as fuel in order to establish the reference against which the other fuels will be compared.

Engine Performance. For the engine performance model depicted in Fig. 2, Table 2 gives the values of the main engine performance parameters at sea-level standard conditions for the maximum continuous (MCP), take-off (TOP), and one engine

Table 1 Fuels considered and their properties

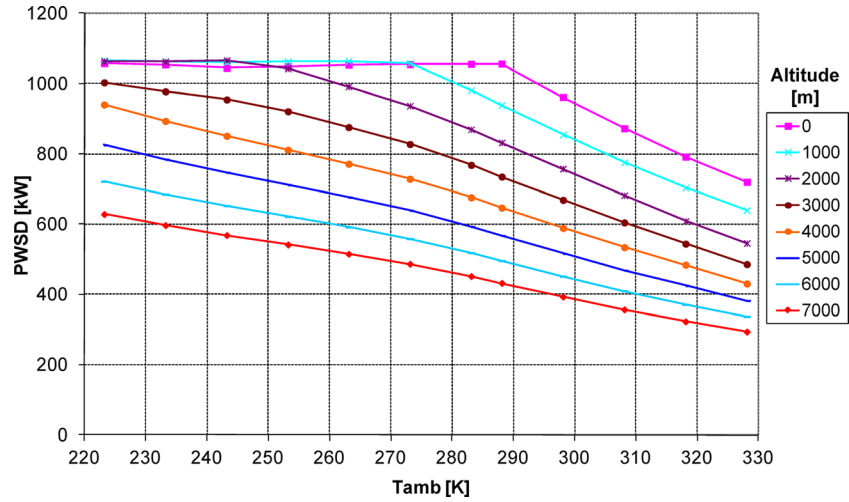| Fuel	H:C ratio	LHV (MJ/kg)		Density (kg/m^3)	
Jet-A	1.917	43.12	(Ref.)	801.0	(Ref.)
Synjet (FT) [9]	2.166	43.94	(+1.9%)	762.4	(−4.8%)
S8 (FT-GTL) [10]	2.169	43.90	(+1.8%)	756.0	(−5.6%)
Jatropha algae (HRJ) [4]	2.119	44.20	(+2.5%)	748.0	(−6.6%)
50% Jet-A + 50% Jatr./alg. blend [4]	2.017	43.70	(+1.34%)	780.0	(−2.6%)
Biodiesel (soybean) [11]	1.855	38.00	(−11.9%)	880.0	(+9.9%)

Fig. 4 Variation of shaft power delivered with ambient temperature and altitude for maximum continuous power rating
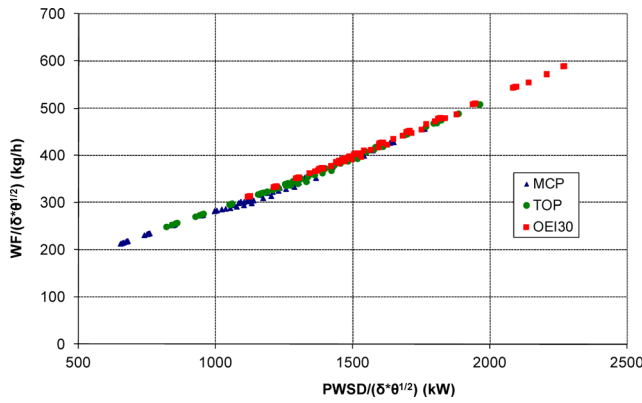

Fig. 5 Engine fuel flow characteristic

inoperative for 30 s (OEI30) power ratings. As already mentioned in the previous section, a fixed power turbine rotational speed is assumed at all conditions (21,000 rpm) which results in a shaft delivered rotational speed of 6,000 rpm through the engine gearbox (corresponding to a fixed helicopter rotor speed).

For control purposes, an upper limit is imposed on the gas generator rotational speed for each power rating. For the MCP rating, Fig. 4 shows how the shaft power delivered by the engine (PWSD) varies with ambient temperature (Tamb) at different altitudes. This means that PWSD remains constant at lower altitudes as Tamb decreases.

If the corrected fuel flow rate is plotted against the corrected shaft power delivered for all three ratings and for altitudes from 0 to 7000 m and Tamb from 223 to 328 K (example helicopter environmental operational limits), the graph presented in Fig. 5 is obtained. This shows the unique fuel flow-PWSD relationship for this engine. Hence, if the engine power is known at certain environmental conditions then the corresponding fuel flow rate can be estimated from this curve.

The specific fuel consumption (SFC) variation with PWSD is illustrated in Fig. 6. This is obtained at sea-level standard
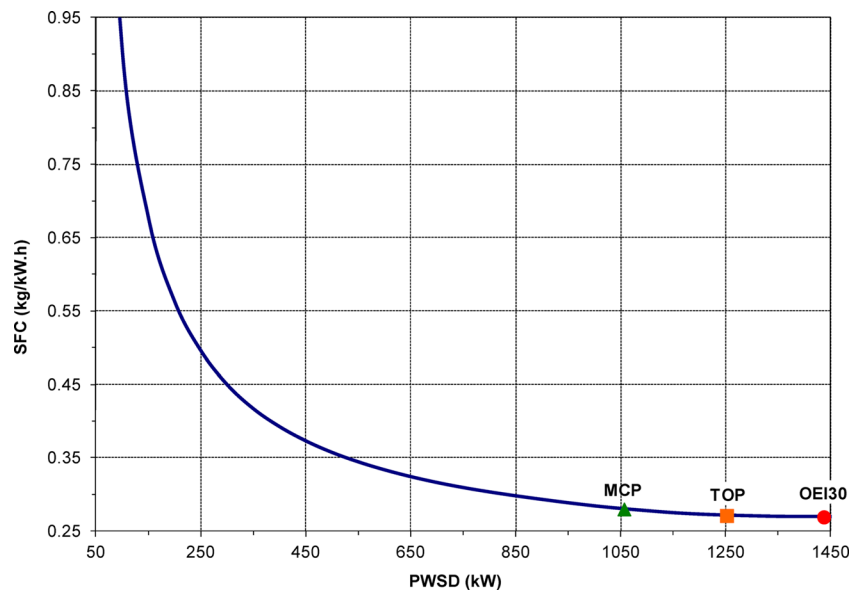

Fig. 6 Engine specific fuel consumption at SL/STD

Table 3   Helicopter parameters

Parameter	Symbol	Value	Units
Maximum take-off weight	MTOW	7400	kg
Weight empty	WE	4105	kg
Fixed useful load[a]	FUL	200	kg
Fuel capacity	VFu	1.45	m^3
Number of engines	Neng	2	-
Number of rotor blades	Nb	4	-
Main rotor diameter	D	15.2	m
Main rotor blade chord	c	0.49	m
Main rotor solidity	σ	0.08	-
Rotor blade tip speed	U	223	m/s
Rotor speed	NR	280	rpm
Equivalent flat plate area	SCx	3.0	m^2
Power extraction	Pex	10	kW

[a]Crew + trapped oil and fuel.

conditions. The three power ratings are also indicated on the graph. At these higher power conditions SFC remains almost constant (see also Table 2) but increases sharply at lower powers. For the example helicopter considered in this study, the cruise power

at sea-level is approximately 50% of that at TOP rating resulting in a SFC value of around 0.33 kg/(kWh).

Helicopter Performance. The basic parameters of the helicopter considered in this study are presented in Table 3. The statistical method presented in [13] is employed in order to determine typical values. The basis of these calculations is the helicopter maximum take-off weight (MTOW).

For this helicopter and for its MTOW, the estimated variation of total power required with forward speed (Vx) at different altitudes (standard atmosphere) is shown in Fig. 7. The power available from the two engines at MCP (assumed constant with Vx) is also included in the plot for the sea-level (SL) and 5000 m cases. There is a significant decrease in excess power with increasing altitude over the entire range of speeds. Although at higher altitudes less power is required at higher speeds at the same time less power is available from the engines compared to that at sea-level.

From the total power required at various altitudes and forward speeds and the engine power available at the same conditions, the maximum rate of climb of the helicopter can be obtained. This is shown in Fig. 8 for the sea level and 2000 m cases. As altitude increases the maximum rate of climb decreases (less excess power available) and this maximum value occurs at a higher forward
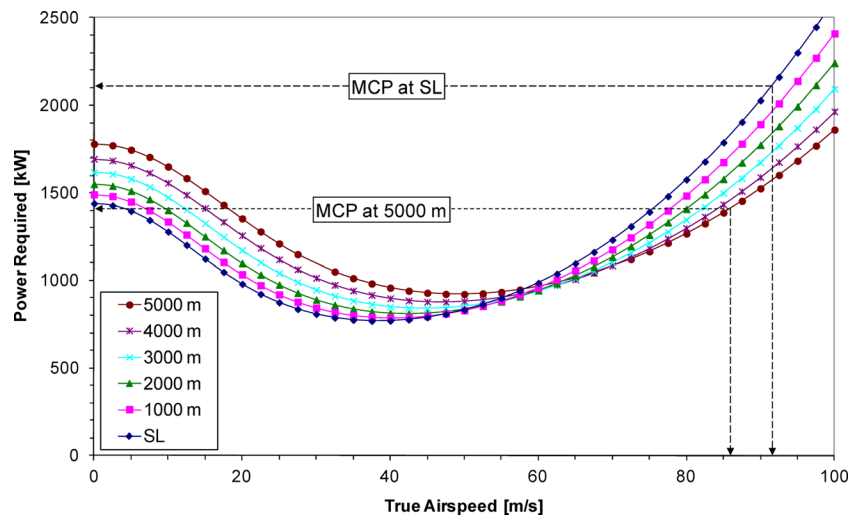

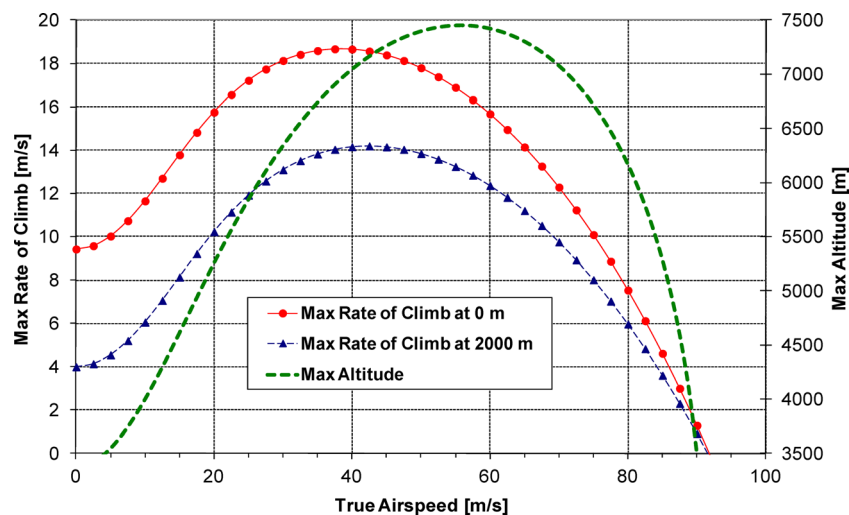**Fig. 7   Helicopter power required at various altitudes (MTOW/STD)**

Fig. 8   Helicopter max rate of climb at 0 and 2000 m and max altitude/ceiling (MTOW)

Journal of Engineering for Gas Turbines and Power
NOVEMBER 2012, Vol. 134 / **111401-5**

Downloaded From: https://gasturbinespower.asmedigitalcollection.asme.org on 06/29/2019 Terms of Use: http://www.asme.org/about-asme/terms-of-use
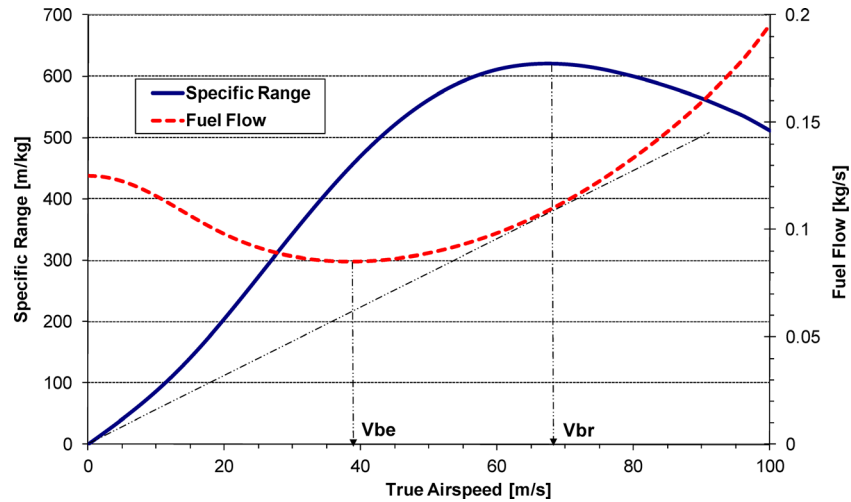
Fig. 9   Helicopter specific range at MTOW and SL/STD

velocity. Also shown in the figure is the maximum height the helicopter can fly at different speeds. This curve is generated by running the integrated model for different values of Vx and determining the value of altitude for which there is no excess power (power required = power available).

For creating the payload-range diagram for this helicopter, the relationship between specific range and helicopter weight needs to be established. The integrated model is employed to find the engine fuel flow rate required for different values of helicopter weight (from empty to MTOW) and forward speeds. Then the specific range is simply the speed divided by the total fuel flow rate for the two engines [14]. The variation of specific range (SR) with speed is presented in Fig. 9 for MTOW and sea-level standard conditions. The maximum SR value occurs at a speed known as velocity for best range (Vbr). This can also be found by drawing a tangent line to the fuel flow rate curve from the origin [8]. The value of Vbr increases with increasing helicopter weight and altitude. Another important value of velocity is that corresponding to minimum fuel consumption. This is known as velocity for best endurance (Vbe). At this speed, the power required is minimum hence excess power available is maximum and the maximum rate of climb can be accomplished (see also Figs. 7 and 8). Both velocities are marked on the graph.

The payload-range diagram shown in Fig. 10 is constructed assuming that the helicopter mission consists of a 2-min warm up period at MCP, cruising at Vbr (at sea-level) and landing with 10% fuel reserve [14]. It is assumed that the fuel burned during the take-off, climb, and descent phases is negligible. The full fuel line is made up from three points (maximum, half of maximum, and zero payload cases) where SR is estimated at the mission mid-point weight (take-off weight minus warm up and half-cruise fuel weight). The zero range payload value is found by subtracting WE and FUL from MTOW.

Having established the engine and helicopter performance for Jet-A, the use of alternative fuels can now be assessed.

Effects of Alternative Fuels. For each of the five alternative fuels considered in this study, the engine model is executed by specifying the power presented in Table 2, for each of the three power ratings. The effect on engine fuel flow rate is presented in the bar chart of Fig. 11 as a percentage difference from the corresponding Jet-A value. The difference is similar to that of the lower heating value one (see Table 1) between each fuel and Jet-A while it is the same for each of the power ratings. Hence the biodiesel fuel has the largest effect and the blend is the smallest.

All other engine cycle parameters (temperatures, pressures, and mass flow rates) are not affected significantly (less than 0.2%). This is consistent with observations from tests conducted in fixed wing aircraft engines [4, 15]. Figure 12 shows a reduction in the HP turbine entry temperature Tt4 for all cases considered with biodiesel having the largest effect (−3.8 K or −0.26%) at the higher power rating.
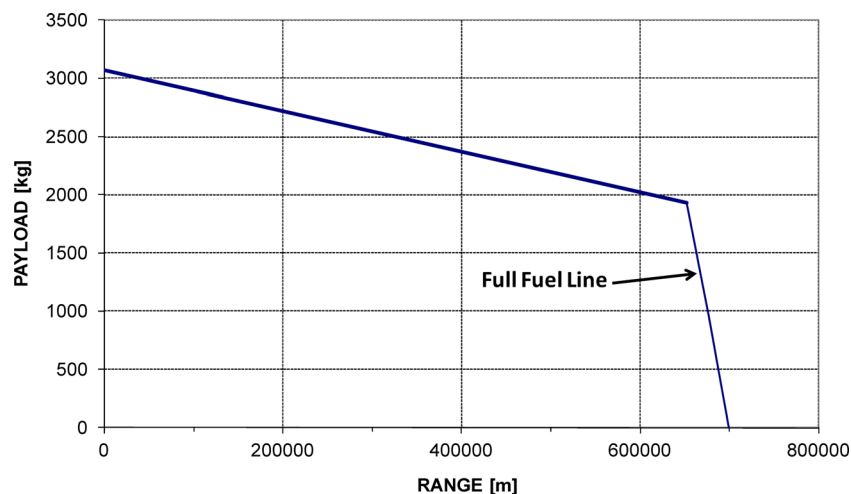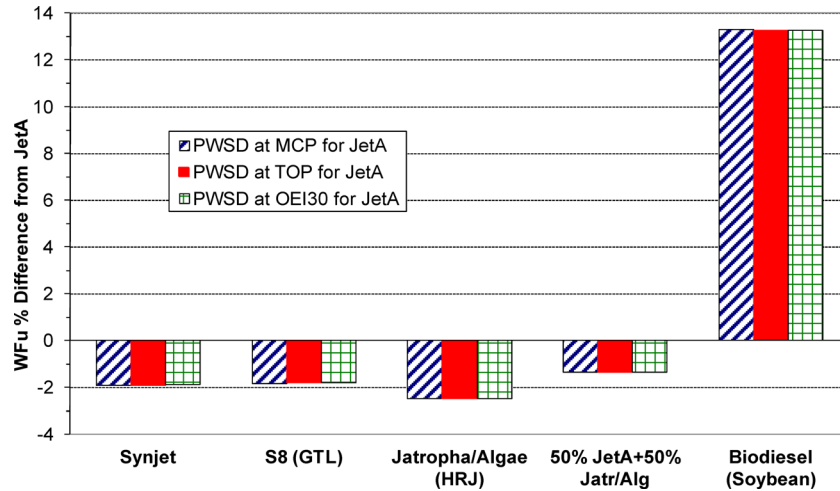

Fig. 10   Helicopter payload-range diagram

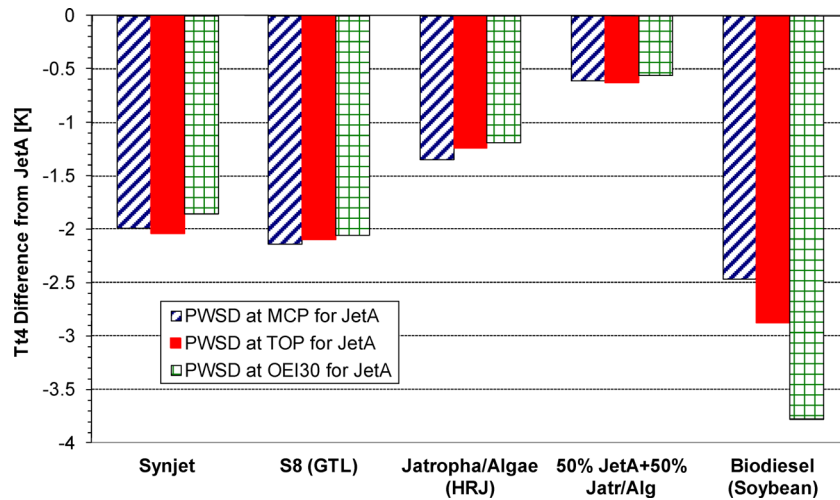**Fig. 11 Effect of alternative fuels on engine fuel consumption**

Fig. 12 Effect of alternative fuels on turbine entry temperature

If instead of a fixed power, a fixed rating is imposed, the effect on shaft power delivered is also less than 0.2%, for all ratings and fuels considered.

The effect of alternative fuels on helicopter operation is studied with the integrated model by simulating the mission described in Table 4. The mission consists of six segments corresponding to the warm up, take-off, climb, cruise, descent, and landing phases. The duration of each phase is further divided into appropriate time intervals (shown in brackets) to improve the accuracy of calculations especially during the climb and descent parts of the mission.

For the same payload and the tanks full of fuel, different take-off weights are obtained for each of the fuels used due to the differences in their densities. The combined effect of different take-off weight and fuel consumption between the fuels is illustrated in Fig. 13 that shows the variation of helicopter weight during the whole mission.

Table 4 Mission description

Segment	Duration in Minutes	
1. Warm up at MCP	2	(1)
2. Take-off from sea-level	2	(1)
3. Climb to 2000 m at Vx = Vbe and Vz, max	2	(0.083)
4. Cruise at Vx = Vbr	40	(1)
5. Descent vertically to sea-level (Vx = 0)	4	(0.083)
6. Land	2	(1)

It should be noted that the value of payload is selected so that with the fuel tanks full with the heavier fuel (biodiesel in this case) the helicopter take-off weight does not exceed its MTOW (7400 kg).

The amount of fuel consumed over the entire mission when using each one of the alternative fuels is depicted in Fig. 14 as a bar chart of percentage differences from that consumed when Jet-A is used. These differences are greater than the corresponding ones of engine fuel consumption presented earlier in Fig. 11. This is due to the different take-off weights considered for each mission. If the same mission is carried out for the same take-off weight (fixed payload and fuel weight) for all fuels used then the change in total fuel consumed over the mission is consistent with that corresponding to the engine fuel consumption alone, as shown in Fig. 14.

The effect of alternative fuels on the helicopter payload-range diagram is obtained by first calculating the specific range—helicopter weight relationship for each of the fuels, using the procedure described in the previous section. The maximum value of specific range is obtained at the same value of forward velocity (Vbr) in all cases since, for a given helicopter, this is only a function of the helicopter weight and the operating altitude. For all fuels, the variation of specific range with helicopter weight is presented in Fig. 15 showing that the jatropha/algae fuel has the highest value due to its LHV. The converse applies for the biodiesel fuel.

The payload-range diagram for each fuel is then obtained assuming the same mission as in the case of Jet-A described previously. Except for the biodiesel fuel, all other fuels allow for a
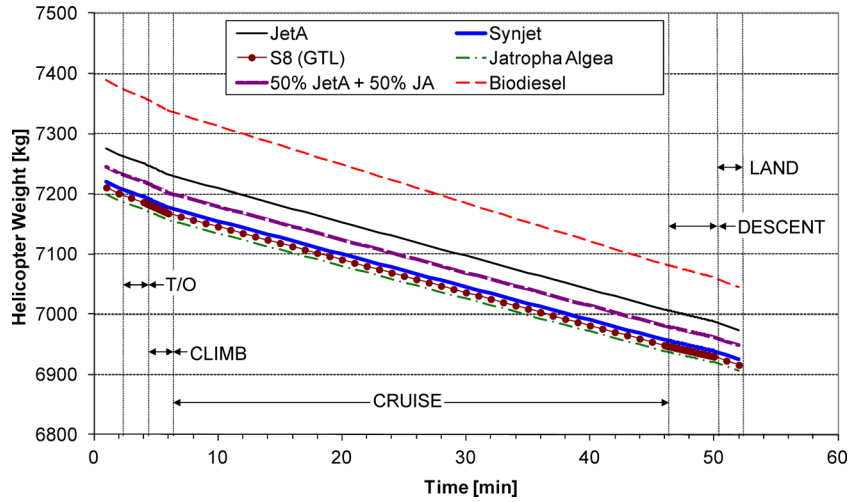
Fig. 13 Helicopter weight variation with time during mission for different fuels (full tanks – fixed payload)
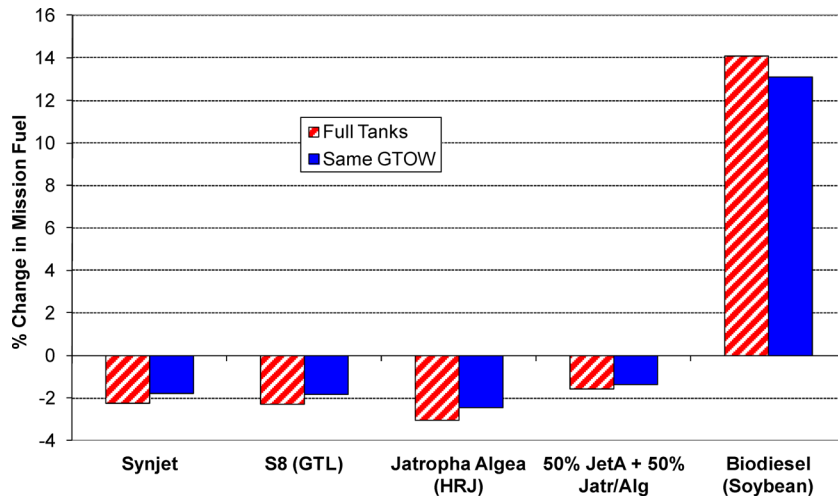

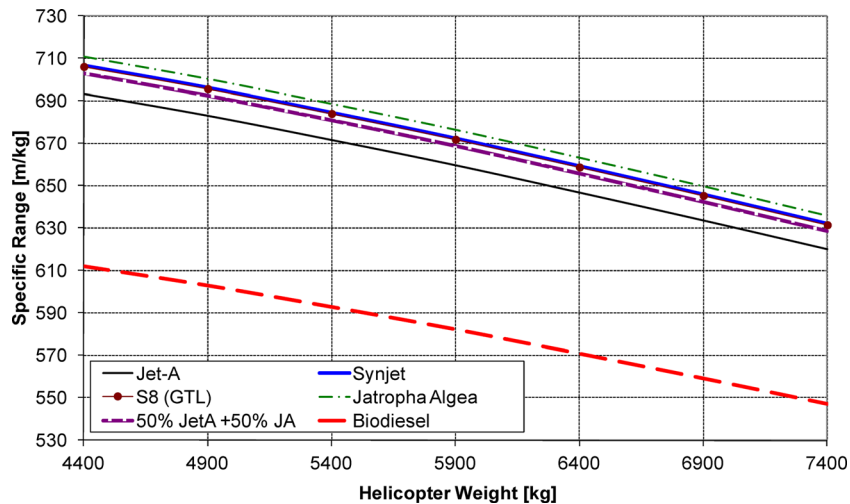**Fig. 14 Effect of alternative fuels on mission fuel**

Fig. 15 Specific range-helicopter weight variation for all fuels

higher payload at a given range compared to Jet-A until they reach their corresponding full fuel value. Then due to their lower density, they result in a lower maximum range value (for zero payload) compared to Jet-A. On the other hand biodiesel always has a

smaller payload compared to the other fuels but due to its higher density results in a higher range compared to some of the other fuels. These results are presented in Fig. 16 in which only the values greater than 500 km are shown. Note that all lines start from
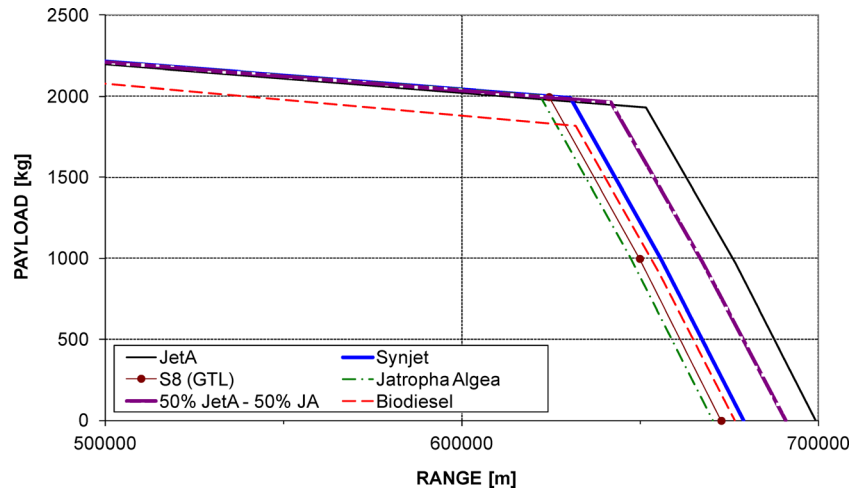
Fig. 16   Effect of alternative fuels on helicopter payload-range characteristics

the same value of payload for zero fuel as that for Jet-A shown earlier in Fig. 10.

Summary and Conclusions

An integrated model of a helicopter and its associated turboshaft model has been created in an object-oriented simulation environment in order to study the effects of alternative fuels on helicopter operation.

The individual and integrated models are firstly described followed by the engine and helicopter performances for the case of a conventional fuel (Jet-A).

Simulations are then carried out for five alternative fuels. For the fuels considered in this study, there are no significant effects on the engine cycle compared to Jet-A except for the fuel flow rate that changes according to the difference of each fuel's lower heating value from the reference one.

Considering the helicopter in a mission, there is an added effect from the differences in density between the fuels that modifies the helicopter's payload-range capability.

Based on the modeling assumptions, the blended fuel appears at the moment as the most suitable choice for the aspects considered in the presented analysis (e.g., taking into account its effects on engine cycle parameters and helicopter operational characteristics) but other parameters should also be taken into account to allow for a more complete assessment (e.g., economics of fuel production, emissions, etc.).

To this end, the method presented herein can be further extended by including models of other disciplines in the existing integrated model (e.g., economics, noise and particulate emissions, etc.). This would allow the required multidisciplinary calculations (including design and optimization) to be performed in a single simulation environment with all the associated benefits that such an approach offers (configuration management control, transparent exchange of information between modules, common modeling standards, flexible mathematical model handling, etc.).

Finally, by creating a library of specific aircrafts (rotary or fixed wing) and a corresponding one with engines (turboshafts, turbofans, etc.) one can perform such studies for various combinations of current and future aircraft-engine models.

Acknowledgment

Nomenclature

CEA = chemical equilibrium with applications
DIT = duct interturbine
FUL = helicopter fixed useful load
GBX = gearbox
GTL = gas-to-liquid
GTOW = gross take-off weight
H/C = helicopter
H:C = hydrogen-to-carbon ratio
HPC = high pressure compressor
HPT = high pressure turbine
HRJ = hydroprocessed renewable jet
IATA = international air transport association
LHV = lower heating value
LPC = low pressure compressor
MCP = maximum continuous power rating
MGB = main helicopter gearbox
MTOW = maximum take-off weight
OEI = one engine inoperative rating
PROOSIS = PRopulsion Object-Oriented SImulation Software
PT = power turbine
PWSD = shaft power delivered
SFC = specific fuel consumption
SL = sea level
SPK = synthetic paraffinic kerosene
STD = standard atmospheric conditions
Tamb = ambient temperature
TOP = take-off power rating
Vbe = velocity for best endurance
Vbr = velocity for best range
Vx = helicopter forward velocity
Vz = helicopter vertical velocity
WE = helicopter empty weight
WF = fuel flow rate
δ = pressure ratio
θ = temperature ratio

References

[1] Acare, 2010, "Aeronautics and Air Transport: Beyond Vision 2020 (Towards 2050)," available at ftp://ftp.cordis.europa.eu/pub/technology-platforms/docs/acare-background-2010_en.pdf
[2] Leahy, J., 2010, "Airbus Global Market Forecast 2010-2029," available at http://www.airbus.com/company/market/forecast/
[3] IATA, 2009, "The IATA Technology Roadmap Report," 3rd ed.

[4] Rahmes, T. F., Kinder, J. D., Henry, T. M., Crenfeldt, G., LeDuc, G. F., Zombanakis, G. P., Abe, Y., Lambert, D. M., Lewis, C., Juenger, J. A., Andac, M. G., Reilly, K. R., Holmgren, J. R., McCall, M. J., and Bozzano, A. G., 2009, "Sustainable Bio-Derived Synthetic Paraffinic Kerosene (Bio-SPK) Jet Fuel Flights and Engine Tests Program Results," Report No. AIAA 2009-7002.

[5] EcosimPro/PROOSIS: Continuous and Discrete Modelling and Simulation Software, 2012, EA Internacional, available at http://www.proosis.com/

[6] Alexiou, A., Baalbergen, E. H., Kogenhop, O., Mathioudakis K., and Arendsen, P., 2007, "Advanced Capabilities for Gas Turbine Engine Performance Simulations," ASME Report No. GT2007-27086.

[7] Grapin, J. C., 2010, Pre-Design Team Engineer, Turbomeca, private communication.

[8] Leishman, J. G., 2006, *Principles of Helicopter Aerodynamics*, 2nd ed., Cambridge University Press, Cambridge, England.

[9] Hermann, F., Hedemalm, P., Orbay, R., Gabrielsson, R., and Klingmann, J., 2005, "Comparison of Combustion Properties Between a Synthetic Jet Fuel and Conventional Jet A1," ASME Report No. GT2005-68540.

[10] Moses, C. A., 2008, "Comparative Evaluation of Semi-Synthetic Jet Fuels—Final Report," CRC Project No. AV-2-04a, available at http://www.crcao.org/reports/recentstudies2008/AV-2-04a/AV-2-04a%20-%20Comparison%20of%20SSJF%20-%20CRC%20Final.pdf

[11] Panchasara, H. V., Simmons, B. M., Agrawal, A. K., Spear, S. K., and Daly, D. T., 2008, "Combustion Performance of Biodiesel and Diesel-Vegetable Oil Blend in a Simulated Gas Turbine Burner," ASME Report No. GT2008-51496.

[12] Gordon, S., and McBride, B. J., 1994, "Computer Program for Calculation of Complex Chemical Equilibrium Composition and Applications," NASA RP1311, National Aeronautics and Space Administration, Washington, D.C., available at http://www.grc.nasa.gov/WWW/CEAWeb/RP-1311.htm

[13] Rand, O., and Khromon, V., 2002, "Helicopter Sizing by Statistics," 58th AHS Forum, Vol. 2, Montreal, Canada, June 11–13, pp. 1155–1176, available at http://ae-www.technion.ac.il/~rapid/site_files/Statistics_example.pdf

[14] Stepniewski, W. Z., and Keys, C. N., 1984, *Rotary-Wing Aerodynamics*, Dover Publications, New York.

[15] Davison, R. C., and Chishty, A. W., 2011, "Altitude Performance of a Turbojet With Alternate Fuels," ASME Report No. GT2011-45132.